

New Durability Assurance Technologies for the Shenzhen–Zhongshan Cross-Sea Bridge

Huanyong Chen ^{1,2} and Di Wang ^{3,*}

¹ Shenzhen–Zhongshan Link Administration Center, Zhongshan 528400, Guangdong Province, China;

² Guangdong Highway Construction Co., Ltd., Guangzhou 510699, Guangdong Province, China;

³ CCCC Highway Consultants Co., Ltd., Beijing 100010, China.

* Correspondence: wangdi@hpdi.com.cn

Abstract: The Shenzhen–Zhongshan Link (Shenzhong Link) is the world's first integrated cross-sea cluster project featuring a "bridge-island–tunnel-undersea interchange", and it is a key national project. The main structures include a 17-kilometer-long sea-crossing bridge and a 6.8-kilometer-long submarine tunnel. The project officially opened to traffic on June 30, 2024, with an average daily traffic volume of approximately 90,000 vehicles. Owing to the alternating loads from vehicles as well as wind, waves, and currents, fatigue issues are prominent. Moreover, the structures are exposed long-term to a marine environment characterized by high temperature, high humidity, and high salinity (fog), leading to severe corrosion problems. Considering that both corrosion and fatigue, as well as their coupled effects, significantly impact structural durability, this paper conducts research on key technologies for ensuring the durability of the Shenzhen–Zhongshan Cross-Sea Bridge, with a particular focus on marine concrete, steel beams, and main cables.

Keywords: Shenzhen–Zhongshan Link; cross-sea bridge; durability; marine concrete; steel beams; main cables

1 Overview

1.1 Project Overview

The Shenzhen–Zhongshan Link has a total length of approximately 24 kilometers, featuring eight lanes in both directions, with a designed speed limit of 100 km/h, and the approved budget is 44.69 billion RMB yuan [1]. The project was located in the core area of the Guangdong–Hong Kong–Macao Greater Bay Area's "9 + 2" city cluster, connecting Shenzhen, Nansha and Zhongshan Districts of Guangzhou. The project officially opened to traffic on June 30, 2024.

The main structures of the project include a 17-kilometer-long sea-crossing bridge and a 6.8-kilometer-long submarine tunnel (as shown in Figure 1). Among these bridges, the main span of the Shenzhong Bridge is 1,666 m, making it the world's largest full offshore sea-crossing suspension bridge [2].



Figure 1 Distribution of major structures

Citation: Chen, H.; Wang, D. New Durability Assurance Technologies for the Shenzhen–Zhongshan Cross-Sea Bridge. *Prestress Technology* 2025, 1, 35–47. <https://doi.org/10.59238/j.pt.2025.01.003>

Received: 26/11/2024

Accepted: 22/01/2025

Published: 30/03/2025

Publisher's Note: Prestress technology stays neutral with regard to jurisdictional claims in published maps and institutional affiliations.



Copyright: © 2025 by the authors. Submitted for possible open access publication under the terms and conditions of the Creative Commons Attribution (CC BY) license (<https://creativecommons.org/licenses/by/4.0/>).

1.2 *Challenges for the Project*

1.2.1 Severe Corrosion Issues

The project is located in a subtropical marine environment characterized by high temperature, high humidity, and high salinity (fog), which significantly exacerbates structural corrosion problems. The region experiences peak temperatures of up to 38.9 °C, with an annual average temperature ranging from 22.3 to 23 °C. The relative humidity can reach 100%, averaging between 78% and 80% annually. The chloride ion (Cl⁻) concentration in seawater at the bridge site is particularly high, reaching 16,734.2 mg/L during low-water periods.

1.2.2 Significant Structural Fatigue Issues

Alternating loads on the structure include those from waves, currents, most notably vehicle and wind loads, which directly impact the fatigue life of steel box girder bridge decks and main cable wires.

As a core strategic passage within the Guangdong–Hong Kong–Macao Greater Bay Area, Shenzhen–Zhongshan Link had exceptionally high traffic volumes after its opening, with an average daily traffic flow of approximately 90,000 vehicles. The coupled effect of saturated traffic flow and the environment will increasingly highlight issues such as corrosion and fatigue cracking of large sea-crossing bridges' steel box girders. The project is located in an area prone to strong typhoons, with significant wind loads. For the control structure, the basic wind speed and flutter check wind speed at the Shenzhen–Zhongshan Bridge site reach 43 m/s and 83.7 m/s, respectively. Alternating wind effects have a considerable influence on structural fatigue.

1.3 *Research Objectives*

In the marine service environment, the combined effects of wave scouring, seawater erosion, and saturated traffic flow significantly exacerbate the degradation of safety for cross-sea transportation infrastructure engineering structures compared with conventional structures. Practical engineering experience indicates that cracking and durability degradation issues in concrete within marine projects are exceptionally prominent. Specifically, high-performance marine concrete has a markedly increased risk of shrinkage cracking compared with traditional concrete. Once cracks form, they accelerate chloride ion penetration and steel reinforcement corrosion, substantially reducing structural durability. The survey results indicate that without necessary crack control and anti-corrosion measures, concrete structures in marine environments can suffer from severe reinforcement corrosion damage within approximately ten years. Therefore, ensuring the crack resistance and durability of concrete structures is critical for the safe operation of cross-sea bridge structures. Additionally, in marine environments, the main cables of suspension bridges are exposed to high temperature, high humidity, and high salinity conditions, with abundant dissolved oxygen and exposure to direct and reflected sunlight. With increasing temperature, the corrosion rate is accelerated, which leads to prominent corrosion problems in the main cable. These problems must be studied and solved in the process of project construction.

In this paper, methods to increase the durability of concrete, steel bridges, and main cable wires through theoretical calculations, experimental analysis, and onsite validation are discussed. The findings provide valuable approaches that can be referenced for future research on the durability of long-span suspension bridges.

2 **Durability Assurance Technology for Concrete Structures**

2.1 *Time-Variant of Service Performance*

Engineering structures in service not only are subjected to environmental erosion but also bear various static loads, dynamic loads, and impact loads. These

loads, acting individually or in combination, can cause macroscopic and microscopic changes in concrete materials, thereby affecting their durability. Through indoor chamber tests and outdoor exposure site tests, the impact of alternating loads on the chloride ion penetration capability of concrete was investigated.

The indoor experimental equipment included a seawater simulation chamber (Figure 2) and an alternating load testing machine. Based on the measured chloride ion concentration values at different depths within concrete structures, it is possible to determine the diffusion coefficient curves of chloride ions in concrete under various loading frequencies and stress levels (Figure 3). The results indicate:

- (1) Under alternating loads, the chloride ion diffusion coefficient is related to the stress level and the alternating frequency (positively correlated).
- (2) Increasing the alternating frequency can significantly enhance the chloride ion diffusion coefficient (on the order of magnitude).



Figure 2 Seawater simulation test chamber

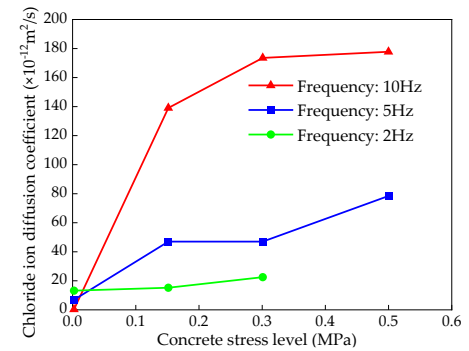


Figure 3 Chloride ion diffusion coefficient under different conditions

Through outdoor exposure tests (Figure 4), the time-variant service performance of the concrete structures was further studied. The results showed that the relationship between the alternating load frequency and the chloride ion diffusion coefficient in concrete can be described by an exponential function (Formula 1):

$$\frac{D_L}{D_0} = 1.06 \cdot e^{0.326 \cdot f} \tag{1}$$

where D_L is the chloride ion diffusion coefficient in concrete under alternating loads, D_0 is the chloride ion diffusion coefficient in concrete without external loading under the same environmental conditions, and f is the alternating load frequency, as illustrated in Figure 5.



Figure 4 Outdoor exposure tests

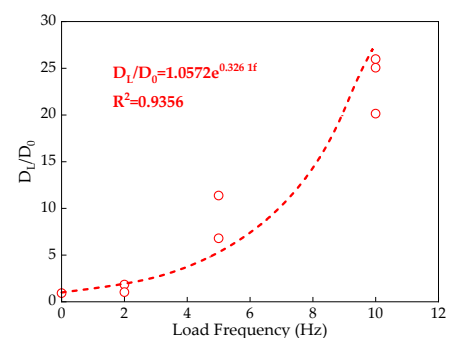


Figure 5 Relationship between the alternating load frequency f and D_L/D_0

2.2 New Technologies for Ensuring Concrete Durability

The technical team of the Shenzhen–Zhongshan Cross-sea Bridge conducted specialized research on concrete durability. In addition to conventional durability

techniques, such as appropriately increasing the thickness of the concrete cover, adding measures such as silane impregnation and epoxy-coated reinforcement bars, optimizing high-performance concrete mix designs, and construction processes, new technologies, such as microcapsule self-healing materials and anti-erosion nanomaterials, have been developed and applied [3].

2.2.1 Microcapsule Self-Healing Materials

Microcapsule technology is a technique that uses a healing agent as the core and a polymer as the shell to create core-shell structured microcapsules. This technology has been widely applied in the pharmaceutical, food, and printing industries. In the construction industry, adding microcapsules to concrete has a significant positive effect on maintaining its mechanical properties. Not only can it accurately locate defects within the cement matrix, but it also enables the automatic repair of microcracks. The process of microcapsule self-healing in concrete is illustrated in Figure 6. When microcracks appear in the cement matrix, under the force exerted by the crack tips, the shell of the microcapsules ruptures, releasing the healing agent, which prevents internal microcracks from propagating further within the structure.

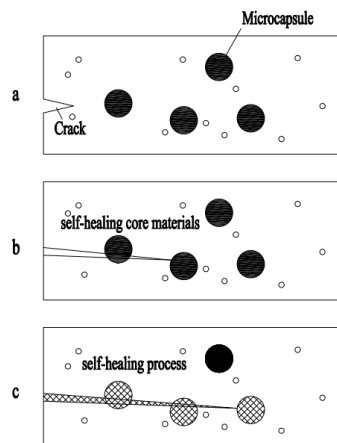


Figure 6 Process of microcapsule self-healing in concrete

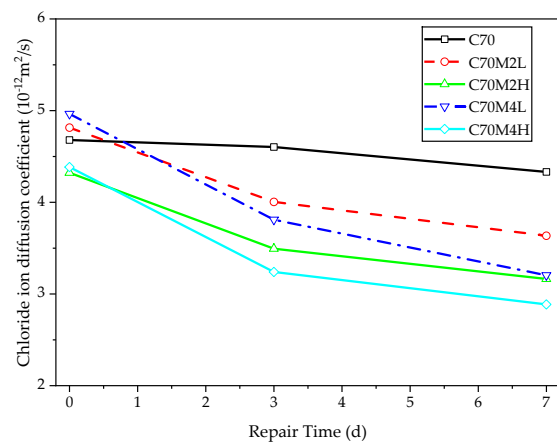


Figure 7 Chloride ion permeability repair efficiency

The project team, which used high-performance concrete with a microcapsule content of less than 5% as an example, verified the repair performance of microcapsule self-healing materials on concrete structures through laboratory and onsite tests. The research results indicate the following: (1) Strength repair: microcapsule self-healing concrete demonstrates good self-repair efficiency in a natural environment, with the highest strength recovery rate reaching 16%. (2) Chloride Ion Permeability Resistance Repair: Both natural curing and high-temperature curing in a curing chamber can enhance the chloride ion permeability resistance of high-performance concrete. The repair effect is better under natural curing conditions; the highest repair rate at 7 days is approximately 50% (as shown in Figure 7).

2.2.2 Anti-Erosion Nanomaterials

Anti-erosion nanomaterials are a new type of nanomaterial based on a hydration response mechanism. It has strong hydrophobic properties and anti-medium transmission properties, which can effectively inhibit the transmission and diffusion of water and corrosive ions in concrete and improve the durability of concrete structures. The nanomaterial precursors are obtained by heating a mixture of organic solvents and organic acids to 50–150 °C, adding an appropriate amount of polyether, and reacting with a catalyst for 10–16 hours. Subsequently, esterification reactions are used to prepare anti-erosion nanomaterials with varying chain lengths, water

solubilities, and strong dispersions (as shown in Figure 8). On this basis, laboratory tests and field validation experiments (with the concrete mix proportions detailed in Table 1) were conducted to investigate the impact of anti-erosion nanomaterials on the compressive strength and water absorption rate of concrete.

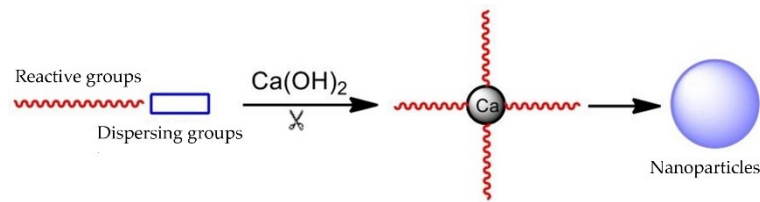


Figure 8 Schematic diagram of the hydrolysis of anti-erosion nanomaterials and the generation of nanoparticles

Table 1 Material mixing ratios of C45 concrete (Unit: kg/m³)

P II 52.5 Cement	Fly ash	Mineral powder	Sand	Stone	Water	Water reducer	Anti-erosion nanomaterials
248	101	101	759	1,048	123	1.5	30

The results show that anti-erosion nanomaterials have no negative effect on the compressive strength of concrete but can significantly reduce the water absorption of concrete. With increasing dosages of anti-erosion nanomaterials, the reduction in water absorption by the concrete increases, effectively improving the densification of bridge concrete. The water absorption rate is often used to evaluate the resistance of concrete to medium penetration due to its close relationship with concrete durability. As shown in Table 2, the 3-day water absorption rate of concrete containing anti-erosion nanomaterials meets the durability design criterion of less than 1.0%, thereby enhancing the overall durability of the concrete.

Table 2 Mechanical properties and durability performance indicators

Items	Reference concrete	Concrete with anti-erosion nanomaterials
28-day compressive strength (MPa)	61.6	63.3
3-day water absorption rate (%)	1.49	0.63

3 Durability Assurance Technology for Steel Box Girders

The Shenzhen–Zhongshan Link includes a total bridge length of 17 kilometers, comprising two main bridges: the Shenzhen–Zhongshan Bridge and the Zhongshan Bridge. Both the Shenzhong Bridge (cross-sections shown in Figure 9), the Zhongshan Bridge, and most of the approach bridges are constructed using steel box girder structures, with approximately 280,000 tons of steel used in the bridges. The orthotropic steel bridge decks cover an area of approximately 380,000 m² and face the global challenge of fatigue cracking, particularly at the welds connecting the U-ribs to the deck plates and the U-ribs to the diaphragm plates, which are especially prone to fatigue cracking.

The factors contributing to fatigue cracking in steel box girders can be categorized into external and internal causes.

- (1) External causes: Repeated vehicle loads cause cumulative damage at critical locations. This issue is particularly pronounced under the saturated traffic volume conditions of the Shenzhen–Zhongshan Link.
- (2) Internal causes: Unreasonable structural systems, construction details, and manufacturing methods result in initial defects, which inherently reduce the fatigue design strength of the structure from the outset.

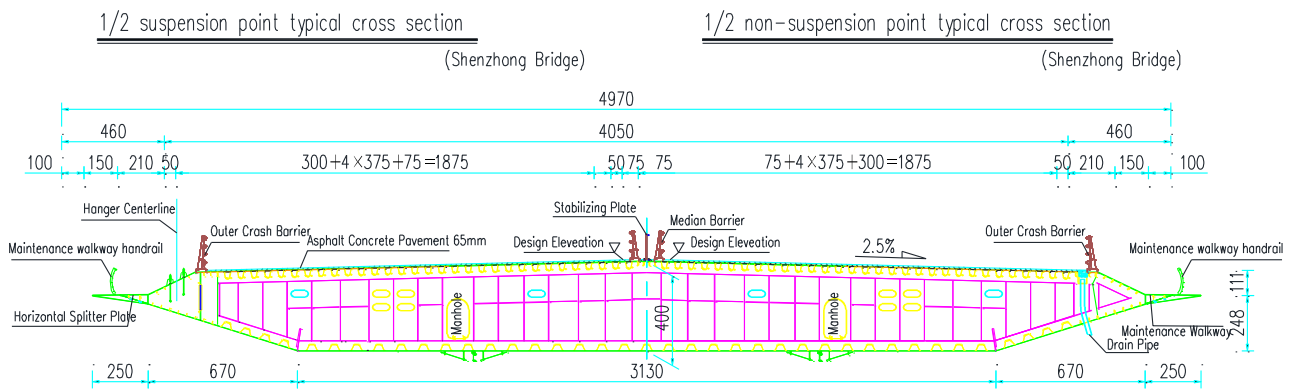


Figure 9 Steel box girder cross section of the Shenzhong Bridge

This project team focuses on the connection welds between U-ribs and bridge deck plates, which are the most critical areas susceptible to fatigue damage. Through full-scale tests on nine plate elements, a comprehensive theoretical analysis model was established for the nucleation and propagation of microshort cracks as well as the propagation of macrolong cracks. A high-quality, full-penetration welding joint and technique for U-ribs (Figure 9) was developed, significantly reducing the initial microcrack size in the welds from 300 μm to less than 20 μm (Figure 10). The fatigue design strength of the welded details between the longitudinal ribs and top plates improved substantially from 80 MPa to 125 MPa. This achieves full penetration and inspectability of the welds, maximally eliminating initial defects and enhancing the fatigue durability of orthotropic steel bridge decks.



Figure 10 High-quality fully penetrated weld joints for U-ribs

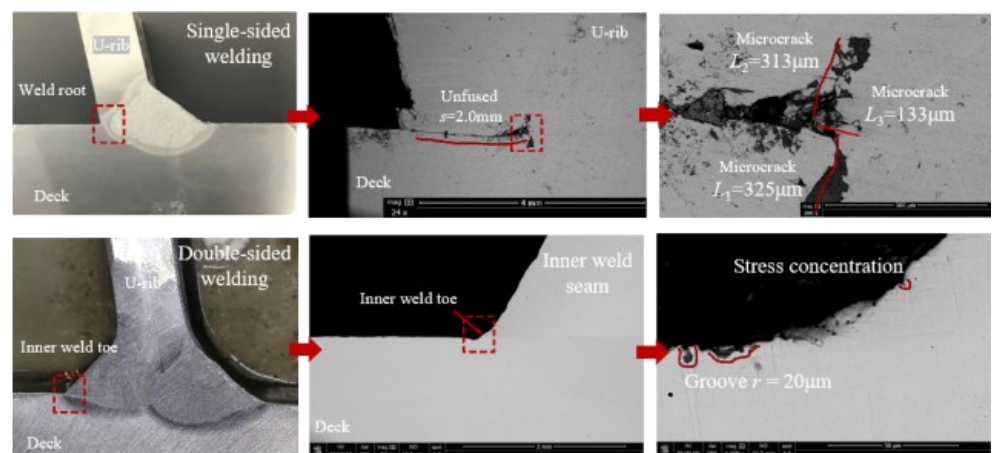


Figure 11 Comparison of the technical quality of single-sided welding and automated double-sided submerged arc welding

The welds connecting the U-ribs to the diaphragm plates experience extremely complex stress, with significant welding deformation and residual stress. This makes them more susceptible to stress concentration and initial welding defects, leading to stress amplitudes under loads that exceed the fatigue limit values. Consequently, this can result in fatigue damage and even the formation of fatigue cracks. Various national standards stipulate that no weld access holes should be set at the welding positions between the top plate and longitudinal ribs as well as the diaphragm plates. However, weld access holes are allowed at the welding positions between the diaphragm plates and the bottom of the U-ribs (see Figure 12). Setting openings at these welding positions can effectively reduce the stress levels of these structural details, and different opening forms have varying effects on the stress state of fatigue-prone areas in the diaphragm plates. For this project, a comparative analysis was conducted on four different opening forms (see Figure 12).

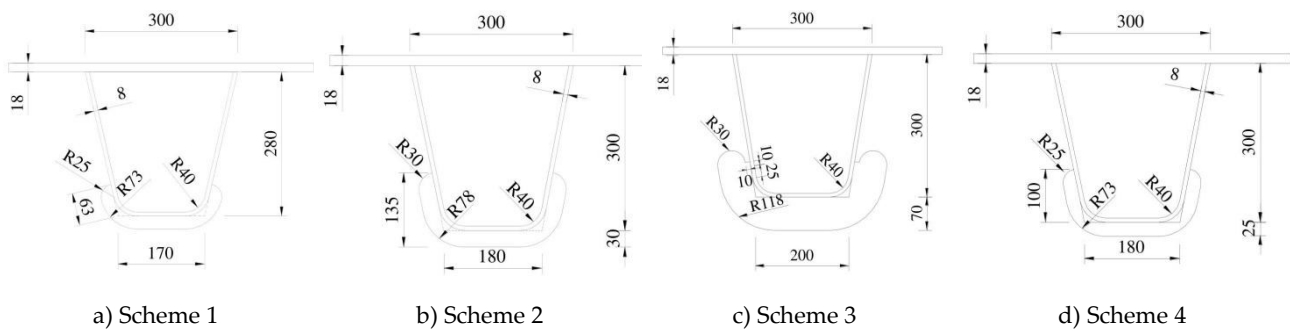


Figure 12 Design parameters of the four different opening forms (Unit: mm)

There are three primary fatigue cracking modes at the intersection of the longitudinal ribs and diaphragm plates:

- (1) Cracks initiate at the end of the weld (weld toe), where the longitudinal rib connects to the diaphragm plate, and propagate along the web of the longitudinal rib (marked as D1-1).
- (2) Cracks also originate at the weld toe but extend along the diaphragm plate (marked D1-2).
- (3) Cracks start from the arc-shaped opening position of the diaphragm plate and continue to propagate within the diaphragm plate (marked D2).

For the different opening schemes shown in Figure 12, the maximum principal tensile stress values for these fatigue details are listed in Table 3:

Table 3 Maximum principal tensile stresses of typical fatigue susceptible details in different hole types (Unit: MPa)

Opening forms	Scheme 1	Scheme 2	Scheme 3	Scheme 4
Fatigue detail D1	39.57	41.67	32.27	41.28
Fatigue detail D2	44.56	36.54	47.98	36.75

Based on the calculation results of Schemes 1 to 4, the maximum principal tensile stress for the intersection fatigue detail D1 between the longitudinal ribs and diaphragm plates, from smallest to largest, is as follows: Scheme 3, Scheme 1, Scheme 4, and Scheme 2. For the arc-shaped opening position fatigue detail D2 in the diaphragm plates, the maximum principal tensile stress, from smallest to largest, is as follows: Scheme 2, Scheme 4, Scheme 1, and Scheme 3. Ultimately, Scheme 4 was selected as the optimal choice.

4 Durability Assurance Technology for the Main Cable

The Shenzhen–Zhongshan Cross-sea Bridge is equipped with two main cables, each with a diameter of 1053 mm, and cable clamps with a diameter of 1066 mm.

Each main cable consists of 199 strands, with each strand consisting of 127 high-strength steel wires, each having a diameter of 6 mm and a nominal tensile strength of 2,060 MPa. To adapt to the high-temperature, high-humidity, and high-salinity environment of the Lingdingyang Sea area, the main cable wires are coated with a zinc–aluminum multicomponent alloy. Additionally, a three-layer protection system is employed: a Z-shaped wire + wrapping tape + dehumidification system.

4.1 Main Cable Steel Wires

The main cables are the lifelines of suspension bridges and cannot be replaced within their 100-year design lifespan. As the world’s largest span fully offshore sea suspension bridge, the main cables of the Shenzhen–Zhongshan Cross-sea Bridge are subjected to even more severe environmental conditions, requiring greater durability assurance. Therefore, the project team conducted research on the corrosion fatigue failure mechanisms of the main cable wires in marine environments and developed ultrahigh-strength $\phi 6-2060$ (6 mm diameter, nominal strength of 2060 MPa) main cable wires along with corresponding zinc-aluminum-rare earth (magnesium) ternary alloy coating protection technology. Corrosion tests revealed that the durability lifespan of these wires is three times greater than that of hot-dip galvanized wires (Figure 13).

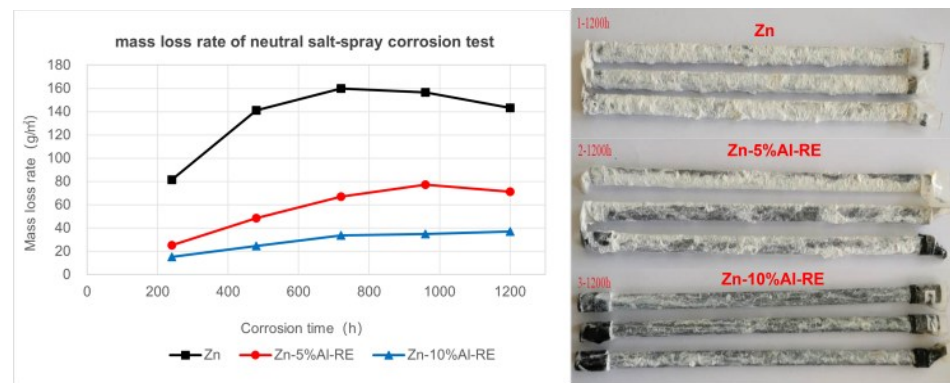


Figure 13 Comparison of neutral salt spray test results for different alloy-coated steel wires

The project team conducted 2 million conventional fatigue tests. According to project requirements, the main cable wires needed to withstand 2 million fatigue cycles without failure under stress conditions with an upper limit of $0.45 \sigma_b$ (where σ_b is the tensile strength of the wire) and a stress amplitude of 410 MPa. The test results (see Table 4) show that the conventional fatigue performance of the Shenzhong Bridge's main cable wires meets the requirements specified in the standard "Hot-dip zinc or Zinc–Aluminum Coated Steel Wires for Bridge Cables" (GB/T 17101–2019).

Table 4 Number of stress cycles used in conventional fatigue tests

Test group number	Fatigue stress conditions				Total number of fatigue stress cycles N
	Stress amplitude	Maximum stress	Minimum stress	Average Stress	
	σ_a (MPa)	σ_{max} (MPa)	σ_{min} (MPa)	σ_m (MPa)	
1	460	927	467	697	2.0×10^6
	460	927	467	697	2.0×10^6
	460	927	467	697	2.0×10^6
2	410	927	517	722	2.0×10^6
	410	927	517	722	2.0×10^6
	410	927	517	722	2.0×10^6

Test group number	Fatigue stress conditions				Total number of fatigue stress cycles <i>N</i>
	Stress amplitude	Maximum stress	Minimum stress	Average Stress	
	σ_a (MPa)	σ_{max} (MPa)	σ_{min} (MPa)	σ_m (MPa)	
3	360	927	567	747	2.0×10^6
	360	927	567	747	2.0×10^6
	360	927	567	747	2.0×10^6

To address the simultaneous corrosion and fatigue effects on the main cables, a special dry–wet alternating corrosion–fatigue coupled test was performed, in which an SF06 salt spray chamber and a 100 kN axial tensile fatigue testing machine were used to conduct dry–wet alternating corrosion–fatigue coupled tests. Under different stress amplitudes, the following cycle was adopted: fatigue stress cycle → high-temperature salt spray wet corrosion → room-temperature salt spray deposition dry corrosion + fatigue stress cycle → high-temperature salt spray wet corrosion → room-temperature salt spray deposition dry corrosion + fatigue stress cycle. This cycle of uneven corrosion and fatigue alternations continued until the steel wire experienced corrosion–fatigue fracture, and the number of fatigue cycles to failure and the corrosion state of the wire surface were recorded. The process is shown in the following diagram:

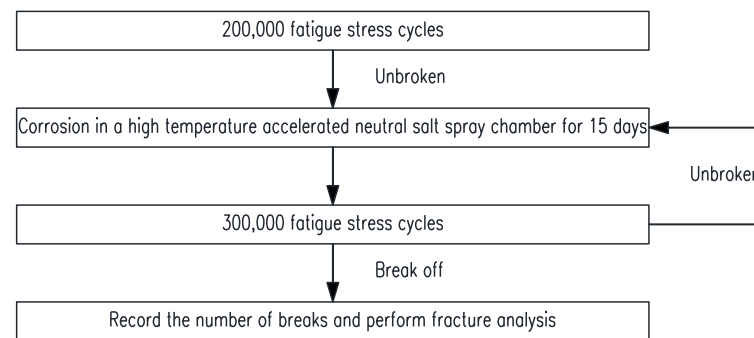


Figure 14 Processes of dry–wet alternating corrosion and fatigue cycle coupling tests

The results of the dry–wet alternating corrosion–fatigue coupled test (Table 5) show that at a stress amplitude of 360 MPa, the $\phi 6$ –2060 steel wire with a zinc–10% alloy coating endured 1.97 million stress cycles, approaching 2 million cycles.

Table 5 Number of stress cycles used for the dry–wet alternating corrosion and fatigue cycle coupling tests

Test group number	Fatigue stress conditions			Total number of fatigue stress cycles <i>N</i>	Dry corrosion time of salt deposition at room temperature (h)	Wet corrosion time of salt spray at high temperature (h)
	Maximum stress	Minimum stress	Stress amplitude			
	σ_{max} (MPa)	σ_{min} (MPa)	σ_a (MPa)			
1	927	467	460	1.29×10^6	96	1,440
	927	467	460	1.32×10^6	96	1,440
	927	467	460	1.33×10^6	96	1,440
2	927	517	410	1.36×10^6	96	1,440
	927	517	410	1.37×10^6	96	1,440
	927	517	410	1.37×10^6	96	1,440

Test group number	Fatigue stress conditions			Total number of fatigue stress cycles N	Dry corrosion time of salt deposition at room temperature (h)	Wet corrosion time of salt spray at high temperature (h)
	Maximum stress σ_{max} (MPa)	Minimum stress σ_{min} (MPa)	Stress amplitude σ_a (MPa)			
3	927	567	360	1.96×10^6	144	2,160
	927	567	360	1.96×10^6	144	2,160
	927	567	360	1.97×10^6	144	2,160

4.2 Cable Clamp Airtightness

To address the issue of potential air leakage in cable clamp positions, a triple-seal structure has been implemented at the straight seams, circumferential seams, and bolt positions [4] (Figure 15). At the straight seams, a rubber spring seal strip adaptable to a gap ranging from 15 mm to 35 mm between half-clamps has been developed (Figure 16). For the circumferential seams, an extended multisawtooth sealing structure is proposed for the interface between the ends of the cable clamp and the main cable, enhancing the quality of the seal (Figure 17).



Figure 15 Triple-seal structure of the cable clamp

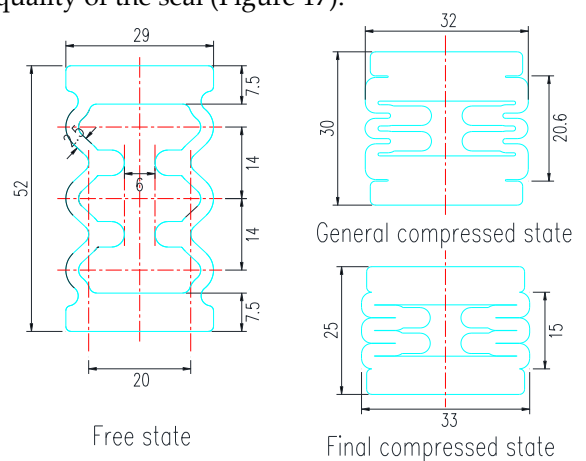


Figure 16 Straight seam rubber spring sealing strip

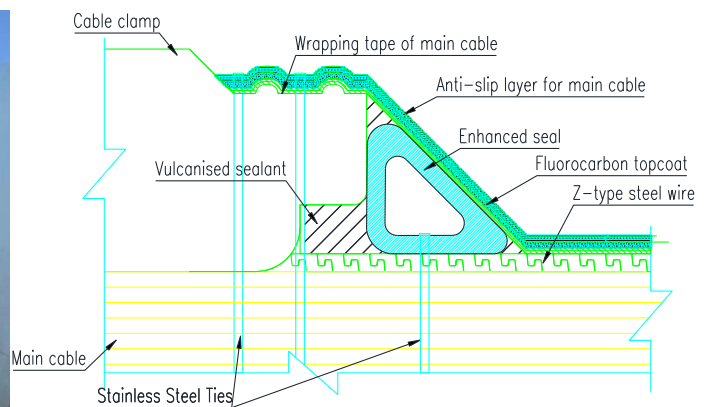


Figure 17 Sealing sample of the cable clamp ring seam

To verify the effectiveness of the new cable clamp airtightness solution, the project team conducted pressure retention tests on both the traditional airtight solution (Scheme 1) and the new airtight solution (Scheme 2). The test process was as follows:

- (1) After the cable clamps were assembled, the sealant was allowed to cure.

- (2) Gas was introduced to perform the pressure test.
 - (3) Once the internal gas pressure of the cable clamps reached the set requirement of 6,000 Pa, the inlet valve is closed, and the pressure is maintained for 30 minutes.
 - (4) During the pressure retention period, check if there is any pressure drop. If a drop is detected, all areas coated with soapy water are inspected for sealing issues, and any leakage points are identified.
 - (5) Reseal any identified leakage points, wait for the sealant to cure, and then reperform the pressure test.
 - (6) The above steps are repeated until no new leakage points can be found, and then the final pressure test is conducted under this state.
- The results are shown in Table 6 below:

Table 6 Results of the gas pressure tests

Scheme	Observation time and result of gas pressure					
	30 min	3 h	5 h	8 h	14 h	24 h
Scheme 1	No change	Drop 0.5 kPa	Drop 2.5 kPa	Drop 4.0 kPa	Drop 5.5 kPa	Drop 6.0 kPa
Scheme 2	No change	No change	No change	No change	No change	No change

Through repeated testing, the new airtight solution (Scheme 2) can maintain pressure for 24 hours without any drop. This sealing method provides better overall airtightness for the cable clamps.

4.3 Main Cable Dehumidification System with Intelligent Perception Adjustment Function

To monitor the temperature and humidity inside the main cables, the Shenzhen–Zhongshan Link has, for the first time in the world, installed four smart strands within the main cables. Specifically, one steel wire each from the central 100# strand and the surrounding 38#, 42#, and 175# strands were selected (see Figure 18), with fiber Bragg grating (FBG) temperature and humidity sensors installed along their entire length at intervals of 1 to 1.5 meters. Using a combination of FBG sensor technology and ultralong strand encapsulation techniques, this project has developed 3000-meter-class ultralong smart strands for the first time, providing foundational data for scientific dehumidification. The smart strands are led out from the anchorages at both ends of the main cables, and special thermal insulation measures are employed to avoid the impact of the 480 °C high temperature during the casting of the anchors.

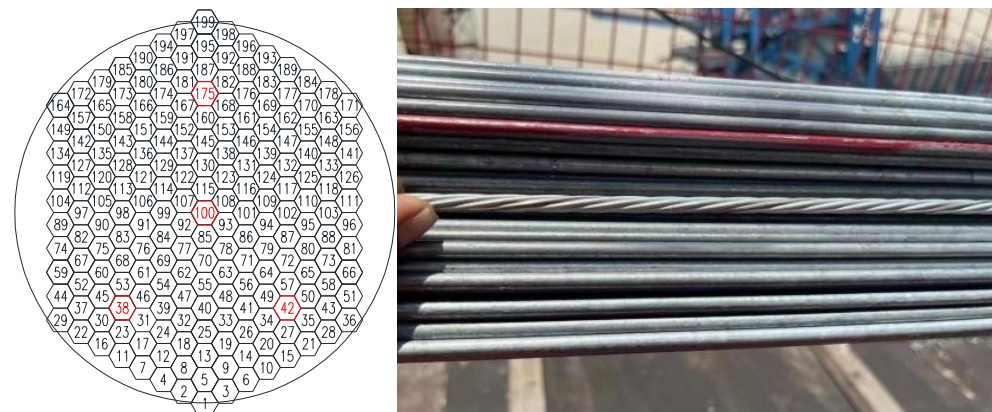


Figure 18 Smart strand section and steel wire

As shown in Figure 19, after preprocessing (filtering) the monitoring data of the temperature, humidity, and main cable corrosion rate, the data are input into an

intelligent analysis system. After the correlations between corrosion and humidity and between dehumidification and environmental factors are analyzed, control parameter commands are output to the intelligent dry air regulation system; this enables intelligent adjustment of the main cable humidity, ensuring that the humidity at the air preparation station outlet and the inlet clamp is $\leq 40\%$ RH and that the humidity at the exhaust clamp is $\leq 50\%$ RH.

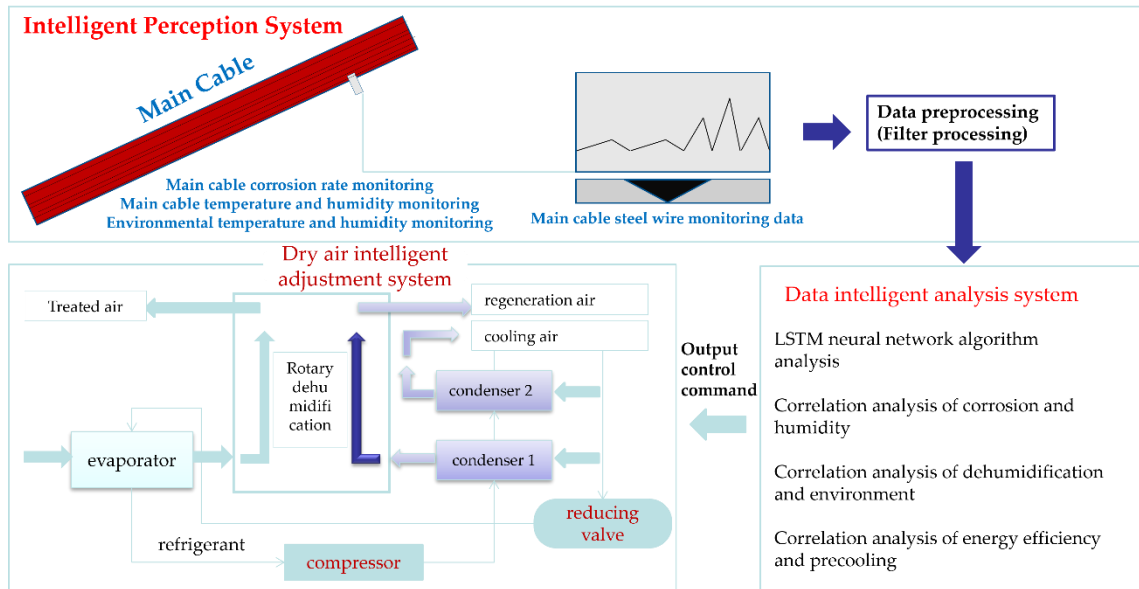


Figure 19 Main cable dehumidification system with intelligent perception and adjustment functions

Through the above measures, from opening to traffic on June 30, 2024 to September 30, the humidity inside the main cables was reduced to below 40% (as shown in Figure 20) within just three months, which is approximately half the time required for similar projects.

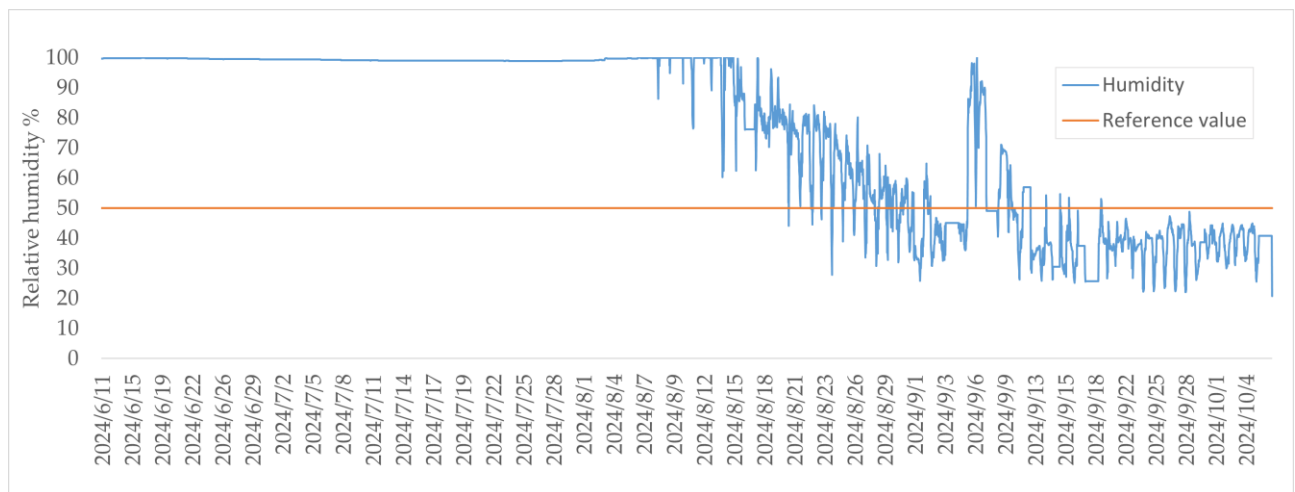


Figure 20 Humidity change at the exhaust clamp in the middle of the main span

5 Conclusions

The Shenzhen–Zhongshan Link spans the Pearl River estuary and, after opening to traffic, is expected to handle an average daily traffic volume of approximately 90,000 vehicles. The structures face significant challenges from both strong corrosion and high fatigue, making durability a prominent issue. After years of technical research and breakthroughs, the project has achieved a series of results in new

technologies for ensuring the durability of concrete and steel structures (steel box girders and main cables), ensuring low-carbon operation after the project's completion. The technical results of the project's durability assurance are as follows:

- (1) Concrete structure: The time-dependent performance laws of concrete in marine environments were revealed. New technologies, such as microcapsule self-healing and anti-erosion nanomaterials, have been developed and applied.
- (2) Steel box girder: Full penetration high-quality welding joints for U-ribs and internal welding technology were developed. The fatigue design strength of the welds between the U-ribs and deck plates was significantly increased from 80 MPa to 125 MPa.
- (3) Main cables: The world's highest strength 2,060 MPa main cable wires were developed. A comprehensive approach combining new ternary alloy coatings, airtight cable clamps, and intelligent dehumidification systems was adopted to ensure a 100-year service life for the main cables.


Conflict of interest: All the authors disclosed no relevant relationships.

Data availability statement: The data that support the findings of this study are available from the corresponding author, Wang, upon reasonable request.

References

1. Song, S.S.; Chen, W.; Jin, W.; Xia, F.; Fu, B. Key Technologies and Challenges of Shenzhong Link. *Tunnel Construction* **2020**, *40*, 143-152, doi:10.3973/j.issn.2096-4498.2020.01.019.
2. Chen, H.; Song, S.; Zhang, H.; Huang, D. Key Manufacturing Technology of 2060 MPa Zn-Al-Mg Alloy Coated Steel Wire Strands Utilized in Lingdingyang Bridge. *Bridge Construction* **2022**, *52*, 21-27, doi:10.3969/j.issn.1003-4722.2022.05.004.
3. Wang, K.; Su, Z.; Song, S.; Liu, J.; Xiong, J. *Shrinkage Crack Control and Durability Guarantee Technologies for Mass Concrete In Marine Environment*, 1 ed.; China Communication Press Co., Ltd.: 2023.
4. Chen, H.; Xu, J.; Li, P.; Zhang, X. Optimization of Main Cable Dehumidification and Corrosion Resistance of Lingdingyang Bridge of Shenzhen-Zhongshan Link. *Bridge Construction* **2023**, *53*, 1-7, doi:10.20051/j.issn.1003-4722.2023.04.001.

AUTHOR BIOGRAPHIES

	<p>Huanyong Chen M.E., Graduated from South China University of Technology in 2003. Research Direction: Bridge and Tunnel Engineering, BIM and Digital Work. Email: 58568000@qq.com</p>		<p>Di Wang B.E., Graduated from Jilin University in 2009. Working at CCCC Highway Consultants Co., Ltd. Research Direction: Long-Span Bridge Design. Email: wangdi@hpdi.com.cn</p>
---	--	--	---